Elevated expression of TDP-43 in the forebrain of mice is sufficient to cause neurological and pathological phenotypes mimicking FTLD-U

Kuen-Jer Tsai,[1] Chun-Hung Yang,[2,3] Yen-Hsin Fang,[2] Kuan-Hung Cho,[4] Wei-Lin Chien,[5] Wei-Ting Wang,[2] Tzu-Wei Wu,[2] Ching-Po Lin,[4] Wen-Mei Fu,[5] and Che-Kun James Shen[2,3]

[1]Institute of Clinical Medicine, National Cheng Kung University, Tainan 704, Taiwan
[2]Institute of Molecular Biology, Academia Sinica, Taipei 115, Taiwan
[3]Institute of Genome Sciences, [4]Institute of Neuroscience, National Yang-Ming University, Taipei 112, Taiwan
[5]Institute of Pharmacology, National Taiwan University, Taipei 100, Taiwan

TDP-43 is a multifunctional DNA/RNA-binding factor that has been implicated in the regulation of neuronal plasticity. TDP-43 has also been identified as the major constituent of the neuronal cytoplasmic inclusions (NCIs) that are characteristic of a range of neurodegenerative diseases, including the frontotemporal lobar degeneration with ubiquitin$^+$ inclusions (FTLD-U) and amyotrophic lateral sclerosis (ALS). We have generated a FTLD-U mouse model (CaMKII-TDP-43 Tg) in which TDP-43 is transgenically overexpressed in the forebrain resulting in phenotypic characteristics mimicking those of FTLD-U. In particular, the transgenic (Tg) mice exhibit impaired learning/memory, progressive motor dysfunction, and hippocampal atrophy. The cognitive and motor impairments are accompanied by reduced levels of the neuronal regulators phospho–extracellular signal–regulated kinase and phosphorylated cAMP response element–binding protein and increased levels of gliosis in the brains of the Tg mice. Moreover, cells with TDP-43$^+$, ubiquitin$^+$ NCIs and TDP-43–deleted nuclei appear in the Tg mouse brains in an age-dependent manner. Our data provide direct evidence that increased levels of TDP-43 protein in the forebrain is sufficient to lead to the formation of TDP-43$^+$, ubiquitin$^+$ NCIs and neurodegeneration. This FTLD-U mouse model should be valuable for the mechanistic analysis of the role of TDP-43 in the pathogenesis of FTLD-U and for the design of effective therapeutic approaches of the disease.

CORRESPONDENCE
Che-Kun James Shen:
ckshen@imb.sinica.edu.tw

Abbreviations used: ALS, amyotrophic lateral sclerosis; CaMKII, Ca^{2+}/calmodulin-dependent kinase II; FTLD-U, frontotemporal lobar degeneration with ubiquitin$^+$ inclusions; GABA, γ-aminobutyric acid; GAD67, glutamic acid decarboxylase 67; GFAP, glial fibrillary acidic protein; LTP, long-term potentiation; mEPSC, miniature excitatory postsynaptic current; MND, motor neuron disease; NCI, neuronal cytoplasmic inclusion; NeuN, neuron-specific nuclear protein; NII, neuronal intranuclear inclusion; pCREB, phosphorylated cAMP response element-binding protein; pERK, phosphorylated extracellular signal-regulated kinase; PGRN, progranulin; Tg, transgenic; UBI, ubiquitinated inclusion.

TDP-43 is a 43-kD protein encoded by one of the multiple splicing isoforms of mRNAs from *TARDBP*, a gene highly conserved in eukaryotes from *Caenorhabditis elegans* to human (Wang et al., 2004). It is an ubiquitously expressed nuclear protein (Wang et al., 2002) with a diverse set of activities in different biological processes, including DNA/RNA binding, repression of gene transcription, and regulation of alternative splicing of the CFTR premRNA (for review see Buratti and Baralle, 2008; Wang et al., 2008a). The characteristics of TDP-43 in cultured hippocampal neurons have suggested that it may play a role in the regulation of neuronal plasticity (Wang et al., 2008b). Loss of TDP-43 in human cells by RNAi resulted in dysmorphic nuclear shape, misregulation of the cell cycle, and apoptosis through the misregulation of the retinoblastoma protein (Ayala et al., 2008). Likely because of its involvement in multiple biological processes, TDP-43 appeared to be required for early mouse embryogenesis (Wu et al., 2010). Interestingly, TDP-43 has been identified as the major disease protein for a range of neurodegenerative diseases, including frontotemporal lobar degeneration with ubiquitin$^+$ inclusions (FTLD-U) and amyotrophic lateral sclerosis (ALS). In particular, it is the signature protein of the ubiquitinated inclusions (UBIs)

The Rockefeller University Press $30.00
J. Exp. Med. Vol. 207 No. 8 1661-1673
www.jem.org/cgi/doi/10.1084/jem.20092164

of these diseases (Arai et al., 2006; Neumann et al., 2006), which include the neuronal cytoplasmic inclusions (NCIs) and neuronal intranuclear inclusions (NIIs; for review see Neumann, 2009; Neumann et al., 2007; Wang et al., 2008a). A causative role of TDP-43 in the pathogenesis of ALS with NCIs has been suggested by the association of >30 different point mutations of the TDP genes with this class of ALS patients (for review see Lagier-Tourenne and Cleveland, 2009).

FTLD-U patients of different subtypes are mainly characterized by ubiquitin$^+$, τ- and α-synuclein$^-$ NCIs (Mackenzie et al., 2006), and, to a lesser extent, NIIs, both of which are also TDP-43$^+$ (Neumann, 2007, 2009; Wang et al., 2008a). FTLD-U is the most common neuropathological subtype of FTLD, which refers to a clinically, genetically, and pathologically heterogeneous group of neurodegenerative disorders (Hodges et al., 2004). FTLD is the second most common form of dementia in people under the age of 65, after Alzheimer's disease, with the prevalence estimated between 3.3 and 25.4 cases per 100,000 people (Ratnavalli et al., 2002). Mutations in the *progranulin* (*PGRN*) and *VCP* genes, respectively, have been identified in a portion of the familial cases of FTLD-U (for review see Cairns et al., 2007; Mackenzie et al., 2006). Clinically, FTLD is characterized by behavioral and/or language dysfunction (Neary et al., 1998). In addition, patients may display movement abnormalities such as Parkinsonism or motor neuron disease (MND; Kertesz et al., 2000; Lomen-Hoerth et al., 2002; Forman et al., 2006). Prominent frontal and temporal lobe atrophy associated with neuronal loss and gliosis are also found in FTLD (Snowden et al., 2007). Currently, there is no drug available for the treatment of FTLD or FTLD-U (Vossel and Miller, 2008).

Despite the rapidly accumulating data on the molecular and cellular properties of TDP-43 in relation to the formation TDP-43$^+$ NCIs or UBIs (Johnson et al., 2008; Winton et al., 2008; Zhang et al., 2009), a causative role of TDP-43 in the pathogenesis of FTLD-U remains undefined. Biochemical analyses have revealed that TDP-43 is promiscuously modified/processed in the affected regions of the brains and spinal cords of the FTLD-U and ALS patients, respectively. In particular, the following TDP-43–derived polypeptides have been detected on Western blots of the urea-soluble extracts from the pathological samples with TDP-43$^+$ UBIs: (a) multiple species of high molecular weight, polyubiquitinated TDP-43; (b) phosphorylated TDP-43 migrating at ∼45 kD; and (c) ∼25- and 35-kD C-terminal fragments of TDP-43 (Arai et al., 2006; Cairns et al., 2007; Kwong et al., 2007; Neumann, 2009; Giordana et al., 2010). In addition, immunohistochemistry analysis of the pathological samples from FTLD-U and ALS patients has revealed the presence of disease cells with NCIs adjacent to TDP-43–depleted nuclei (Arai et al., 2006; Neumann, 2009). The depletion of the nuclear TDP-43 and the formation of the UBIs have been suggested to cause loss-of-function of TDP-43 and cellular toxicity, thus leading to the pathogenesis of FTLD-U and ALS with the TDP-43$^+$ UBIs (Kwong et al., 2007; Mackenzie and Rademakers, 2008; Wang et al., 2008a).

Using a Thy-1 promoter, Wils et al. (2010) generated transgenic (Tg) mice with overexpression of human TDP-43 in the neurons of the central nervous system, in addition to other cell types

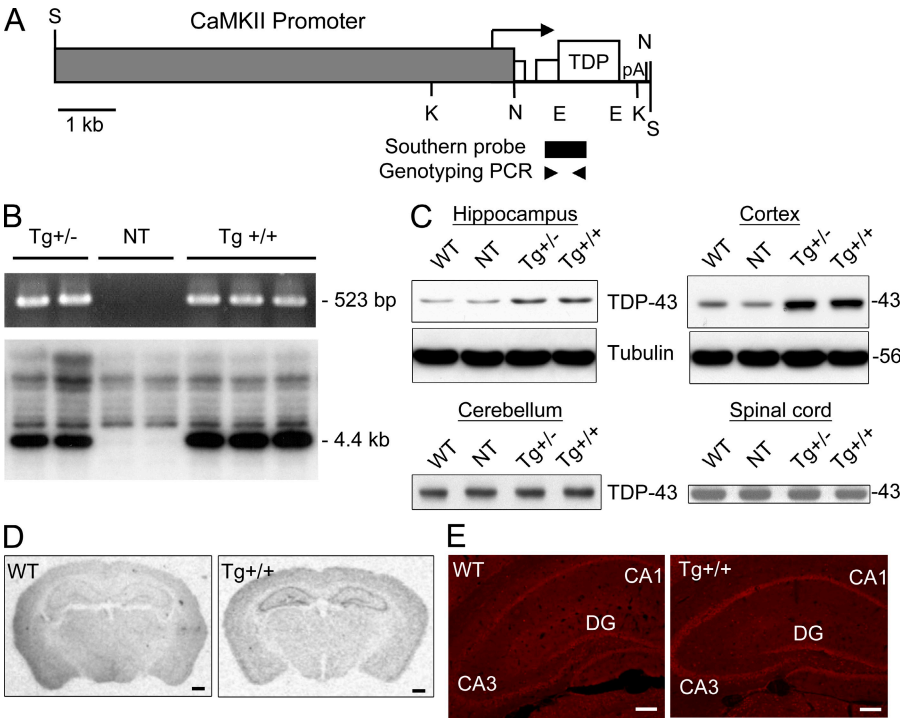

Figure 1. Generation and characterization of CaMKII-TDP-43 Tg mice. (A) Physical map of the CaMKII-TDP-43 fragment for pronuclei injection. The orientation of transcription is indicated by the arrow. The positions of the short hybrid intron derived from an adenovirus splice donor, an immunoglobulin G splice acceptor, and the SV40 poly(A) addition sequence (pA) are indicated. The approximate locations of the Southern blotting and PCR probes are also indicated. Tg mice were identified by the presence of the 4.4-kb KpnI fragment on the Southern blot and the 523-bp PCR band on gel. The restriction sites on the map are as follows: K, KpnI; E, EcoRV; N, NotI; S, SfiI. (B) Genotyping of the Tg mice. The data from PCR (top) and Southern blotting (bottom) analysis of the tail DNAs are exemplified. NT represents the nontransgenic samples. (C) Western blotting of the protein extracts from the hippocampus, cortex, cerebellum, and spinal cord of the WT, NT, and Tg mice, respectively. (D) In situ hybridization patterns of TDP-43 transcripts in the brains of WT and TDP-43 Tg mice (Tg). Bars, 500 µm. (E) Immunostaining patterns of TDP-43 protein in the brains of WT and Tg mice. CA1, CA1 layer; CA3, CA3 layer; DG, dentate gyrus. Bars, 200 µm. Results in B–E are representative of three independent experiments.

in which the Thy-1 promoter is active, including the thymocytes, myoblasts, epidermal cells, and keratinocytes. Degeneration of the cortical/spinal motor neurons associated with a spastic quadriplegia reminiscent of ALS and degeneration of the nonmotor cortical and subcortical neurons characteristic of FTLD were observed in their Tg mice (Wils et al. 2010). Furthermore, cellular aggregates (NCIs and NIIs) containing ubiquitinated and phosphorylated TDP-43, as well as the 25-kD TDP-43 fragment, were detected in association with the disease development and progression of these human TDP-43-overexpressing Tg mice.

In this study, we report the generation of a FTLD-U mouse model with Tg overexpression of TDP-43 in the hippocampus, cortex, and striatum with use of the Ca^{2+}/calmodulin-dependent kinase II (CaMKII) promoter. These Tg mice have developed learning and memory deficits, as well as impairment of their motor functions. The brains of the Tg mice are also characterized with a reduce volume of the hippocampus, gliosis, and TDP-43$^+$, ubiquitin$^+$ NCIs. In interesting connection with the finding that TDP-43 expression is up-regulated in some FTLD-U patients (Chen-Plotkin et al., 2008; Mishra et al., 2007; see Discussion), our data suggest that changes of the homeostatic concentration of TDP-43, in particular the increase of its protein level, in specific types of cells could be a primary cause leading to the development of FTLD-U, and likely other neurodegenerative diseases with TDP-43$^+$ UBIs as well.

RESULTS

Generation of Tg mice

To test whether elevated expression of TDP-43 in the forebrain could be a cause for the generation of the various disease phenotypes as observed in FTLD-U patients, we have constructed Tg mouse lines carrying full-length mouse TDP-43 cDNA under the transcription control of a 8.5 kb promoter region of the CaMKII gene (Mayford et al., 1996; Fig. 1 A). Genotyping by PCR and Southern blotting was used to identify the transgene-positive mice of the founders and their progenies, as exemplified in Fig. 1 B. DNA samples from both the heterozygotes$^{+/-}$ and homozygotes$^{+/+}$ of the Tg mice gave a 523 bp band in the PCR analysis and a 4.4 kb fragment in the Southern blotting analysis. Neither band was present in the non-Tg (NT) samples (Fig. 1 B). The identities of the homozygotes of the Tg mice were also confirmed by breeding them with the NT mice (unpublished data).

Three independent Tg lines were generated, and they exhibited similarly elevated levels of TDP-43 expression (approximately twofold higher than the NT mice) as directed by the CaMKII promoter in the cortex and hippocampus, which was detected by Western blotting analysis (Fig. 1 C, top left and right). The TDP-43 protein levels in the cerebellum and spinal cord of the Tg mice were similar to those of the WT mice (Fig. 1 C, bottom left and right). Note the higher levels of TDP-43 in the hippocampus and cortex samples from the Tg mice. The similar levels of the TDP-43 protein in the hippocampus or cortexes of the Tg$^{+/-}$ and Tg$^{+/+}$ mice might be caused by a feedback regulatory mechanism on the protein level because the TDP-43 mRNA level of the Tg$^{+/+}$ mice was approximately twofold of that of the Tg$^{+/-}$ mice (Fig. S1). The details of this observation require further examination. As confirmed by in situ hybridization experiments, the WT mice exhibited basal signals, whereas the TDP-43 Tg mice showed higher signals in both the hippocampus and cortex (Fig. 1 D). As expected, both the endogenous (Fig. 1 E, left) and the overexpressed, exogenous TDP-43 proteins (Fig. 1 E, right) were present in the hippocampus mainly in the neuronal layers, as shown by immunohistochemical staining.

Impaired performances of the TDP-43 Tg mice in the Morris water maze and fear-conditioning tasks

We first used the water maze task to evaluate whether overexpression of TDP-43 in the hippocampus and cortex affected the learning/memory of the mice. As shown, the 2-mo-old Tg$^{+/+}$ mice exhibited significantly impaired performance in the

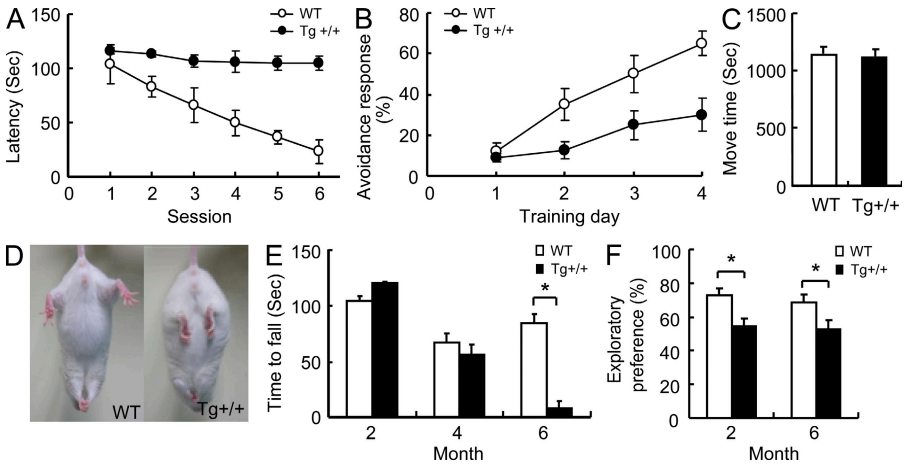

Figure 2. Behavioral performances of CaMKII-TDP-43 Tg mice. (A) Water maze tests of 2-mo-old WT and TDP-43 Tg mice. The learning/memory capabilities are expressed as the latencies exhibited in six consecutive sessions of the test. Results represent the mean ± SEM of three independent experiments (n = 20 mice/group). (B) Comparison of the cognitive functions of 2-mo-old WT and Tg mice in the fear-conditioning task. (C) Locomotor activity test of 2-mo-old WT and Tg mice. Results in B and C represent the mean ± SEM of three independent experiments and (n = 16 mice/group). (D) Abnormal limb-clasping of a 6-mo-old Tg mouse in comparison to a WT mouse when suspended by their tails. Results are representative of five independent experiments. (E) Rotarod tests of WT and Tg mice. The time until drop from the rotating rod (20 r.p.m.) are shown for mice at 2, 4, and 6 mo of age. (F) Performance of mice in 1-h novel object recognition tests. The results represent the mean ± SEM of three independent experiments (n = 10 mice/group). *, $P < 0.05$.

test (compare the latencies of the Tg mice to those of the WT mice in Fig. 2 A, and to the NT littermates as shown in Fig. S2). Because the heterozygous$^{+/-}$ and homozygous$^{+/+}$ Tg mice exhibited similar extents of impairment in their learning/memory capabilities (Fig. S2), we used the homozygous Tg$^{+/+}$ mice for all subsequent behavior tests and other experimental analyses. As shown in Fig. 2 B, the impairment of the learning/memory capabilities of the Tg$^{+/+}$ mice were also revealed by the fear-conditioning task. Thus, the data from these two cognition tests together indicated that overexpression of TDP-43 in the hippocampus and cortex of the mice significantly impaired their learning/memory capabilities.

Abnormal limb-clasping and impaired performance of the TDP-43 Tg mice in the rotarod test

We have also analyzed the motor functions of the TDP-43 Tg mice. The Tg mice were born normally and their spontaneous locomotor activities were normal at the age of 2 mo (Fig. 2 C). However, at the age of 6 mo, TDP-43 Tg mice showed limb-clasping reflexes when being suspended by their tails, whereas the control mice extended their limbs (Fig. 2 D). This abnormal reflex was often observed in mouse models of other neurodegenerative diseases, e.g., the Huntington disease (HD; Mangiarini et al., 1996). The mice were further subjected to the rotarod test, and the results indicated that they were severely impaired in motor coordination, balance, and grip strength at the age of 6 mo (n = 10; $P < 0.05$), but not at 2 or 4 mo (Fig. 2 E). The data of Fig. 2 (C–E) showed that the TDP-43 Tg mice developed progressive motor behavioral deficits at the age of 6 mo. Because of the deficiency of the motor functions of the 6-mo-old TDP-43 Tg mice, the mice were also subjected to the novel object recognition test. As shown in Fig. 2 F, the 6-mo-old TDP-43 Tg mice were still deficient in the learning/memory capabilities, just like the 2-mo-old Tg mice.

Electrophysiology analysis of TDP-43 Tg mice

In view of the impairment of the learning/memory of the TDP-43 Tg mice, we have performed electrophysiology analysis of their long-term potentiation (LTP) in comparison to the WT mice. LTP between the Schaffer collaterals and principal CA1 pyramidal neurons in the hippocampal slices prepared from the mice were measured. In correlation with the learning/memory test experiments (Fig. 2), tetanic stimulation of the Schaffer collaterals resulted in robust LTP in slices from the WT mice. However, the slices from the TDP-43 Tg mice had impaired LTP maintenance for 60 min after the LTP induction (Fig. 3 A).

We also recorded the miniature excitatory postsynaptic current (mEPSC) from DIV 12–15 cultured hippocampal neurons (Fig. 3 B). No significant difference in the mEPSC frequencies could be detected (WT, 3.16 ± 0.65; Tg, 4.59 ± 0.83; $P = 0.20$; Fig. 3 B). However, significant difference existed between the mEPSC amplitudes of the WT and Tg mice (WT, 47.30 ± 2.56; Tg, 39.52 ± 2.96; *, $P = 0.03$; Fig. 3 B). Significant difference in the decay time constant (WT, 3.18 ± 0.30; Tg, 4.99 ± 0.25; ***, $P = 0.0006$; Fig. 3 B) was also detected but not the rise time constant (WT, 1.80 ± 0.08; Tg, 1.81 ± 0.04; $P = 0.88$; Fig. 3 B). These data indicated that the receptor gating properties contributing to the EPSC amplitude and that decay kinetics were altered in the TDP-43 Tg mice.

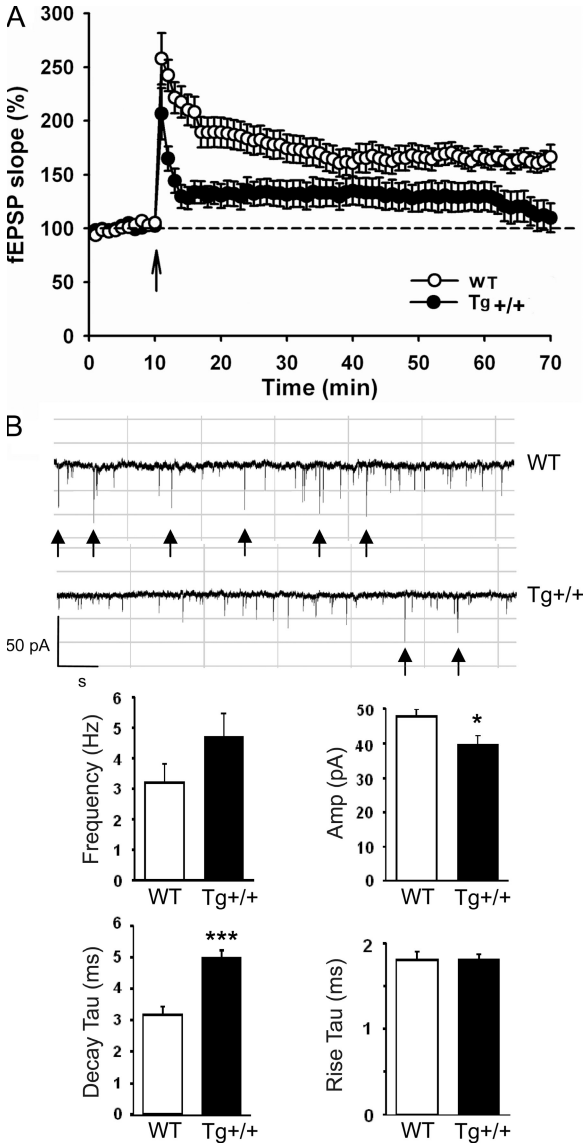

Figure 3. Electrophysiology study of the CaMKII-TDP-43 Tg mice. (A) Attenuated LTP in the hippocampus of 2-mo-old CaMKII-TDP-43 Tg mice. LTP was induced by strong tetanus stimulation in the stratum radiatum layer of CA1. Results represent the mean ± SEM of three independent experiments (n = 18 mice/group). (B) Recording of altered mEPSCs in the primary hippocampal culture of CaMKII-TDP-43 Tg mice. Whole-cell voltage clamp recordings of cultured hippocampal neurons (12–15 DIV) from the WT and TDP-43 Tg mice were performed. Representative traces of the mEPSCs recorded from the neurons are shown on top. The frequencies, amplitudes, decay τ, and rise τ of the mEPSCs are shown in the histograms. *, $P < 0.05$; ***, $P < 0.001$. The scale bars are 50 pA and 1 s, respectively. Results represent the mean ± SEM of three independent (n = 10 mice/group).

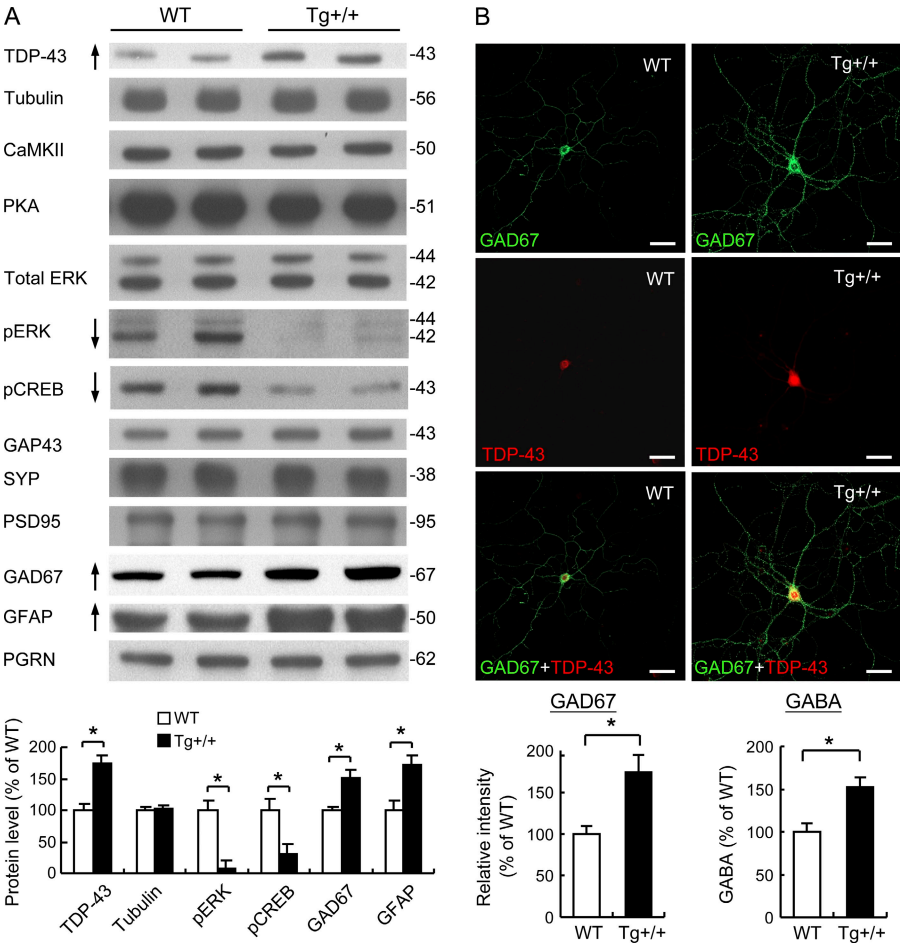

Figure 4. Alterations of the levels of learning/memory-associated proteins in CaMKII-TDP-43 Tg mice. (A) Western blot analysis of different proteins in extracts prepared from isolated cerebral cortex and hippocampus of 2-mo-old WT and Tg mice ($n = 2$ mice/group). Results are representative of three independent experiments. Quantitative analysis of the Western blot data are shown in the lower portion of A. (B) Immunostaining analysis of GAD67 expression and measurement of GABA release. The primary hippocampal neuron cultures of the WT (left) and TDP-43 Tg (Tg, right) mice were double-stained with anti- GAD67 (green) and anti-TDP-43 (red). Bars, 50 µm. The statistical comparison of the relative GAD67 intensities of GAD67+ cells of the WT and Tg mice is shown in the left histogram below the confocal images. The data represent the mean ± SEM of three independent experiments ($n = 20$ mice/group). Shown in the lower right histogram is the statistical comparison of the GABA levels of the WT and Tg mice ($n = 5$; $P < 0.05$).

Decreased levels of phosphorylated extracellular signal-regulated kinase and phosphorylated cAMP response element-binding protein and increased levels of GFAP, GAD67, and GABA in the hippocampus and cortex of TDP-43 Tg mice

In view of the impaired performances of the TDP-43 Tg mice in the learning/memory tests and their lowered LTP (Figs. 2 and 3), we have checked the levels in the hippocampus and cortex of several major candidate proteins known to be involved in different signal transduction pathways regulating learning/memory (Kandel, 2001). Although the protein amounts of CaMKII, protein kinase A, growth-associated protein 43 (GAP43), synaptophysin (SYP), and postsynaptic density 95 (PSD95), respectively, were similar between TDP-43 Tg mice and the WT controls, the levels of both pERK and its downstream target pCREB (Carlezon et al., 2005) in the TDP-43 Tg mice were decreased, as shown by the Western blots and histogram in Fig. 4 A.

It should be noted that the level of *PGRN* in the forebrains of the Tg mice was similar to that of the WT mice (Fig. 4 A). It is not clear at the moment why the level of *PGRN* was not increased in the FTLD-U mouse brains in view of the elevated level of brain GFAP/gliosis in these mice. *PGRN* is expressed in neurons and microglia within the central nervous system and it is elevated in microglia during gliosis (Moisse et al., 2009a,b). Interestingly, in recent models of nerve injury (Moisse et al., 2009a,b), it was found that axotomy caused both increase of TDP-43 and decrease of *PGRN* in the neurons, whereas the level of *PGRN* in the surrounding activated microglia was increased. Thus, likely there could also be a decrease of *PGRN* in the TDP-43–overexpressing neurons of the Tg mouse forebrains, which would compensate for the increase of the *PGRN* amount in the activated microglia. Future experimentation should clarify this point.

Interestingly, the protein levels of the glutamic acid decarboxylase 67 (GAD67) and glial fibrillary acidic protein (GFAP) were also increased, by approximately twofold, in the cortex and hippocampus of the TDP-43 Tg mice. Of the two, GAD67 was known as the principal enzyme for synthesis of the major inhibitory neurotransmitter γ-aminobutyric acid (GABA) in the brain. Its elevated expression in TDP-43 Tg mice was further confirmed by double immunostaining of GAD67 and TDP-43 in the primary neuron cultures from both the Tg mice and the controls (Fig. 4 B). As seen, higher immunostaining signals of GAD67 were present in both the soma and the processes of the neuronal cells of the Tg mice than those of the WT controls (Fig. 4 B, compare the images in the right column to those in the left column), whereas the levels of the neuron-specific nuclear protein (NeuN) were similar between the Tg and control mice (unpublished data). In consistency with the immunostaining data of GAD67, release of the GABA neurotransmitter was also increased in the

forebrains of the TDP-43 Tg mice (Fig. 4 B, bottom right). The results of Fig. 4 suggested that overexpression of TDP-43 impaired the learning/memory of the TDP-43 Tg mice, in part by disrupting the phosphorylation of ERK, but also by up-regulating the inhibitory neurotransmitter GABA.

Neuropathology of the TDP-43 Tg mouse brains

In addition to the behavioral, electrophysiological, and gene expression abnormalities described in Figs. 2–4, the TDP-43 Tg mice also exhibited several neuropathological characteristics similar to those of the FTLD-U patient brains. First, reactive gliosis manifested by increased expression of the astrocytic marker GFAP has been known as a prominent pathological feature of FTLD (Martin et al., 2001; Tan et al., 2005). As shown by Western blotting, the level of the GFAP protein was increased in the TDP-43 Tg mice (Fig. 4 A, bottom). Consistent with this, pronounced increases of the signals of anti-GFAP immunostaining were observed in both the hippocampus (HP) and the cortex (CX) of the $Tg^{+/+}$ mice as compared with the WT controls (Fig. 5 A).

Second, Western blotting analysis revealed the presence of the high molecular weight TDP-43 species, presumably the polyubiquitinated TDP-43, as well as the enrichment of the 25- and 35-kD fragments in the urea-soluble fraction of brain extracts from the 6-mo-old Tg mice (Fig. 5 B). This pattern on the Western blot was much less prominent in samples prepared from the 2-mo-old Tg mice, and it was not observed in those prepared from the WT mice (Fig. 5 B). Note that the high molecular weight TDP-43 species (***) and the 25-kD (*) and 35-kD (**) fragments of TDP-43 are prominent in the 6-mo-old $Tg^{+/+}$ mice, but not in the 2-mo-old mice. The 65-kD band (open triangle) has also been observed by others on immunoblots of extracts from cell lines and from patient lymphocyte lysates (Winton et al., 2008; Corrado et al., 2009), but its significance is not yet clear.

We also performed immunofluorescence staining to examine the subcellular distribution of TDP-43 in the $Tg^{+/+}$ mouse brains in comparison to the WT mice. As shown in Fig. 6 A, TDP-43 was mainly detected in the nuclei, which were positively stained with both anti-NeuN and DAPI, of unaffected neurons of the TDP-43 Tg mouse brains. Notably, however, TDP-43 was absent from the nuclei of neurons with $TDP\text{-}43^{+}$ NCIs (Fig. 6 A, arrows in two leftmost bottom images). The $TDP\text{-}43^{+}$ NCIs were not observed in the brains of the WT mice, as exemplified in Fig. 6 A (right, WT images). Overall, ~15–20% of the neurons in the cortexes of the $Tg^{+/+}$ mice contained the $TDP\text{-}43^{+}$ NCIs. Finally, antiubiquitin immunostaining showed that the $TDP\text{-}43^{+}$ NCIs in the 6-mo-old Tg mouse brains were also positive for the presence of ubiquitin (Fig. 6 B). Overall, the patterns from the proteinopathy analysis of the TDP-43 Tg mice, as displayed in Figs. 5 B and 6, were strikingly similar to those reported for the pathological FTLD-U brain samples with TDP^{+}-UBIs (for review see Forman et al., 2007).

Brain atrophy of the Tg mice

To examine whether brain atrophy developed in the Tg mice as in the FTLD-U patients, we first used MRI to measure the volume of the mouse hippocampus. The result showed that the volumes of the hippocampi of 6-mo-old Tg mice were 17% less than those of the control mice ($n = 5$ for each group; $P < 0.05$). This range of the shrinking was similar to that of the frontal and temporal atrophy observed in some of the FTLD patients (Barnes et al., 2006; Snowden et al., 2007). In parallel with the MRI study, we also examined the brain weights and the cortex neuronal numbers of the mice. The results showed that there was neuronal loss in the 6-mo-old Tg mice. On average, the brain weight of the Tg mice was 12% ($n = 5$; $P < 0.05$) less than the WT mice (Fig. 7 A), and the number of the cortical neurons was reduced by 24% (Fig. 7 B). The neuronal loss might result in part from apoptosis of the neurons in the Tg mouse brains. Indeed, apoptotic nuclei were detected, by TUNEL staining, in the brains of the 6-mo-old $Tg^{+/+}$ mice (Fig. 7 C), and this was accompanied with increases of the amounts of both the total and active caspase-3 (Fig. 7 D).

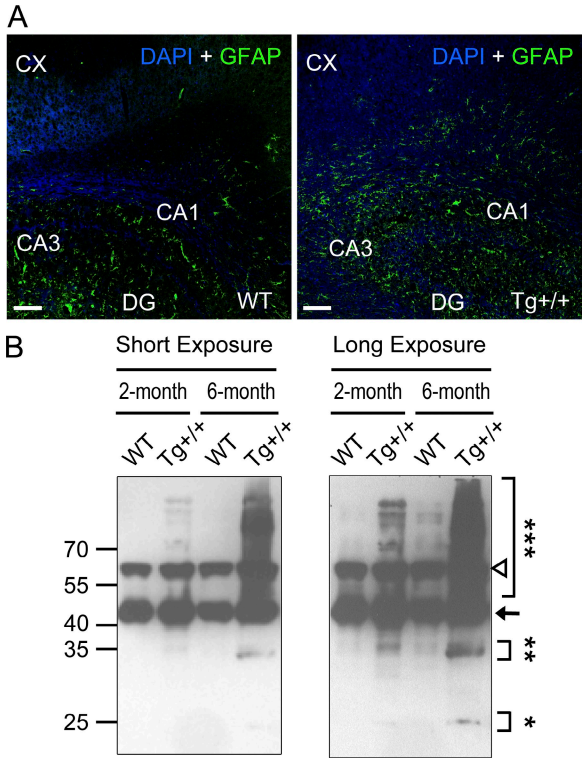

Figure 5. Neurodegeneration of the brains of CaMKII-TDP-43 Tg mice. (A) Representative immunofluorescent images showing GFAP staining (green) in the hippocampus and cortex (CX) of 2-mo-old TDP-43 Tg and WT mice. Nuclei were labeled by DAPI (blue). CA1, CA1 layer; CA3, CA3 layer; DG, dentate gyrus. Bars, 100 µm. (B) Representative Western blotting patterns of the urea-soluble fractions of the brain extracts from the cortexes and hippocampi of the WT mice and $Tg^{+/+}$ mice at 2 mo and 6 mo, respectively. The arrow points to the unmodified form of TDP-43. Results in A–C are representative of five independent experiments.

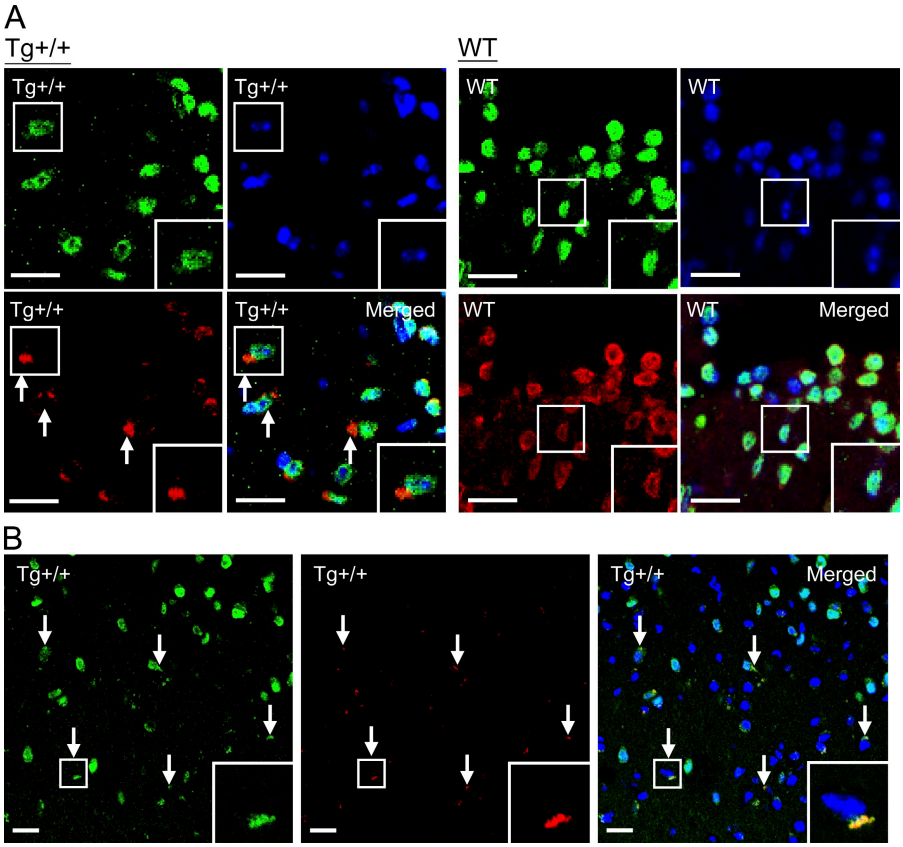

Figure 6. Immunofluorescence staining analysis of TDP-43 distribution in the neurons of the mouse brains. (A) The brain sections of the WT and Tg mice were costained with anti–TDP-43 (red), anti-NeuN (green), and DAPI (blue). TDP-43$^+$ NCIs are indicated by arrows. One neuron each in the Tg$^{+/+}$ and WT samples (boxed) was magnified in the lower right corners (n = 5 mice/group). Bars, 20 µm. (B) Representative immunostaining pattern of a 6-mo-old Tg$^{+/+}$ mouse brain section exhibiting neuronal cells with TDP-43 (green)-containing NCIs that are also positive for the anti-ubiquitin (Ub) staining (red, arrows). High magnification photos of one of the cells with TDP-43$^+$, Ub$^+$ NCIs are shown in the lower right corners . Bars, 20 µm.

Life span of the Tg mice

Finally, we measured the survival rates of the mice. The data, as shown in Fig. S3, indicated that the Tg$^{+/+}$ mice had shorter lifespan, with a mean survival of 495 d, than the WT ones, which had an average survival of 632 d.

DISCUSSION

In this study, we have generated Tg mice with overexpression of mouse TDP-43 in the central nervous systems, including the hippocampus and cortex, under the control of the CaMKII promoter. This promoter has been used before to overexpress other proteins in mice and thus establish different mouse models. However, each of these Tg mouse models exhibits unique phenotypes. For example, overexpression of either CREB (Kida et al., 2002) or NR2b (Tang et al., 1999) enhances the learning/memory capabilities of the mice, which is consistent with the known roles of these factors in learning/memory. On the other hand, overexpression of the methyl-CpG–binding protein 2 (MeCP2) leads to a motor dysfunction phenotype, but it has no effect on the cognitive function of the mice (Alvarez-Saavedra et al., 2007). Noteworthily, CaMKII promoter-directed overexpression does not necessarily affect the mouse behaviors, as exemplified by the Tg mice study of the sulfonylurea receptor, or SUR (Hernandez-Sánchez et al., 2001). In the case of TDP-43, its overexpression has resulted in several molecular, cellular, and phenotypic changes in the mice. These changes include the impairment of learning/memory capabilities, the progressive loss of the motor neuron function, abnormal LTP from the electrophysiological measurement, the increase of gliosis, the alternation of the expression levels of proteins known to be involved in learning/memory, the reduction of the hippocampus volume, and, notably, the TDP-43$^+$-UBI–associated proteinopathological features (Table I). These changes in the CaMKII-TDP-43 Tg mice are strikingly similar to the neurological and pathological features of the FTLD-U patients (Kwong et al., 2007; Vossel and Miller, 2008).

The Tg mice have displayed a pattern of age-dependent loss of the motor function. In respect to this, the FTLD and the MND appear to overlap at several levels, and the FTLD patients share clinical features of MND. It should be noted here that only a portion of the FTLD patients would develop MND (Elman et al., 2008). Development of the motor behavioral deficits in the TDP-43 Tg mice at 6 mo of age (Fig. 2, D and E) parallels the progressive loss of the motor function in the FTLD patients. As deduced from studies of different MNDs, including the ALS (Kwong et al., 2007; Elman et al., 2008), MND could be clinically manifested by signs and symptoms caused by degeneration of the upper motor neurons in the motor cortex, lower motor neurons in the brainstem and spinal cord, or both. However, the size and number of the motor neurons in the spinal cords of the Tg mice are not significantly different from those of the WT (Fig. S4). This is not surprising in view of the forebrain neuron specificity of the CaMKII promoter used by us. Thus, the motor dysfunction of the CaMKII-TDP-43 Tg mice most likely have resulted from damage in the neuronal circuit in the forebrain, which include the not so well-defined rodent motor cortex (O'Leary et al., 2007), and the corticospinal tract, caused by the CaMKII promoter-directed TDP-43 overexpression. It is also possible, but relatively unlikely because of

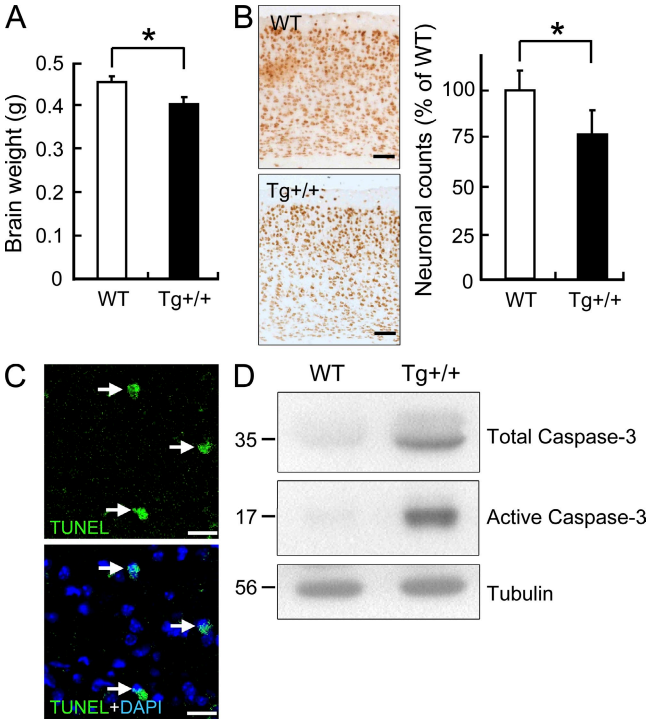

Figure 7. Neuronal loss and apoptosis in the brains of the Tg mice. (A) Reduction of the brain mass of the 6-mo-old Tg mice. Whole brains were dissected and weighed. $n = 5$; $P < 0.05$. (B) Loss of neurons in the cortexes of the Tg mice. Coronal brain sections from 6-mo-old Tg and WT mice were immunostained with anti-NeuN. The average number of the neurons in the cortexes of the Tg mice was compared with that of the WT mice (right; $n = 5$ for each group and $P < 0.05$). Bars, 100 µm. (C) TUNEL assay of the brains of 6-mo-old Tg mice. Apoptotic nuclei are shown in green (arrows) and DAPI staining in blue. (D) Western blots of total brain extracts (cortexes + hippocampi) of 6-mo-old WT and Tg mice showing levels of total and active caspase-3 ($n = 5$ mice/group). Bars, 20 µm.

the CaMKII promoter specificity, that the motor dysfunction originated from some defects in the muscle of the Tg mice. Future detailed analysis of the CaMKII-TDP-43 Tg mice could clarify and differentiate among the aforementioned possibilities.

The CaMKII-TDP-43 Tg mice also exhibit cognitive impairments as reflected by the Morris water maze test (Fig. 2 A), fear conditioning task (Fig. 2 B), novel object recognition test (Fig. 2 F), and LTP electrophysiological recording (Fig. 3). Related to this, the learning/memory deficiency in the FTLD patients is the major factor leading to the dysfunctions of their social behavior and language (Lillo and Hodges, 2009). As a preliminary investigation of the molecular and cellular basis of the effect of the overexpressed TDP-43 on the cognitive functions, we have examined the expression levels of several molecular markers of neuronal plasticity. The results (Fig. 4) indicate that overexpression of TDP-43 has led to the decreases of both p-ERK and p-CREB (Fig. 4), and likely downstream targets such as BDNF (Kandel, 2001). Furthermore, the enhanced gliosis, as observed in the Tg mice (Fig. 5 A), is also known to impair learning/memory (Ridet et al., 1997). Because overexpression of TDP-43 affects a range of biological activities in cell cultures, e.g., transcription (Ou et al., 1995; Wang et al., 2002), alternative splicing (Buratti and Baralle, 2001; Bose et al., 2008), cell cycle progression (Ayala et al., 2008), etc., it is expected that the phenotypes of the Tg mice result from the alternation/ modifications of multiple biological processes as mis-regulated by the overexpressed TDP-43 in the cortex and hippocampus. It should be noted here that one of our previous studies has shown that TDP-43 is distributed in the dendrites of cultured hippocampal neurons as granules/RNA granules (Wang et al., 2008b). However, we have detected no apparent difference in either the distribution pattern or the number of the TDP-43 granules between cultured hippocampal neurons prepared from Tg and WT mice (unpublished data).

In addition to the behavioral phenotypes, the TDP-43 Tg mice also exhibited patterns of neuropathology similar to those of FTLD-U (Arai et al., 2006; Kwong et al., 2007; Neumann, 2009) except for the apparent absence of the phosphorylated 45kD TDP-43 (Fig. 5).Specifically, neurons with TDP-43 depleted nuclei and cytoplasmic TDP-43$^+$, ubiquitin$^+$ inclusions (UBIs) are present in brain sections of the 6-mo-old Tg mice, although they could not be detected in the 2-mo-old Tg mice (Fig. 6 A and B, and Table I). This age-dependent pattern of immunohistochemistry analysis is in good correlation with the immunoblotting data showing the enrichment of the high molecular weight TDP-43 species, presumably the polyubiquitinated TDP-43, and the 25- and 35-kD TDP-43 fragments in the urea-soluble fractions of the brain extracts from 6-mo-old Tg mice (Fig. 5 B and Table I). Thus, it seems that the appearance of the insoluble TDP-43$^+$ UBIs is a priori for the loss of the motor functions, but not the cognitive functions, in the mouse model. On the other hand, the appearance of the NCIs could just be a secondary, age-dependent phenomenon and that some other still unidentified process is responsible for the motor dysfunction of the 6-mo-old Tg mice. The basis for this differential correlation and whether it exists during the development of the human FTLD-U cases require further investigation.

Overall, we have demonstrated that Tg overexpression of TDP-43 in the forebrains of mice leads to development of molecular, cellular, behavioral, and proteinopathological characteristics similar to those identified in FTLD-U. Significantly, there are FTLD-MND patients whose brain TDP-43 mRNA levels are higher than the normal controls (Mishra et al., 2007). A global gene expression study has also found higher level of TDP-43 mRNA in several cases of *PGRN* mutation–positive FTLD-U (Chen-Plotkin et al., 2008). Notably, immunoblotting analysis of lysates from some ALS pathological samples and myopathic muscles with TDP-43$^+$ inclusions has also revealed higher TDP-43 protein levels than the normal controls (Kabashi et al., 2008; Weihl et al., 2008). Thus, our data on the CaMKII-TDP-43 Tg mice suggest that the elevation of the level of TDP-43 protein could be one of the primary causes leading to the pathogenesis of neurodegenerative diseases with TDP-43$^+$ inclusions. After this scenario, different animal models could be generated by

Table I. Summary of the molecular, cellular, and behavioral changes in TDP-43 $Tg^{+/+}$ mice as compared to the WT

		2-mo Tg	6-mo Tg
Cognitive functions			
	Water maze test	decrease	na
	Fear conditioning task	decrease	na
	Novel object recognition test	decrease	decrease
Motor functions			
	Limb-clasping reflex	similar to WT	increase
	Rotarod testing	similar to WT	decrease
LTP		decrease	na
Gliosis	Anti-GFAP staining	na	increase
Expression levels of specific proteins			
	pERK	decrease	decrease
	pCREB	decrease	decrease
	GAD67	increase	increase
	GFAP	increase	increase
Presence on Western blot of urea-soluble fraction of the brain extracts			
	Polyubiquitinated TDP-43	increase	prominent increase
	Phosphorylated TDP-43	absence	absence
	35 kD fragment of TDP-43	increase	prominent increase
	25 kD fragment of TDP-43	absence	presence
$TDP\text{-}43^+$ NCIs adjacent to TDP-43 depleted nuclei in Tg mouse brain sections	Immunohistochemistry	absence	presence
Presence of $TDP\text{-}43^+$, $ubiquitin^+$ NCIs	Immunostaining	absence	presence
Hippocampus volume	MRI measurement	na	decrease
Neuronal loss			
	Brain weight	similar to WT	decrease
	Neuronal counts	similar to WT	decrease
Apoptosis	TUNEL assay	absence	increase

na, not analyzed.

tissue or cell type-specific overexpression of TDP-43 for the basic as well as translational studies of other neurodegenerative diseases with $TDP\text{-}43^+$ UBIs.

It is interesting to compare a few aspects of this study with that by Wils et al. (2010). First, the data from the two studies together provide a strong support for the notion that elevated level of TDP-43 suffices the induction of neurodegeneration in mice, and very likely it is also responsible for the generation and development of the neurodegenerative diseases with TDP-43 proteinopathies, in humans. Second, both studies have identified TDP-43–containing NCIs and activation of caspase-3 in association with neuronal apoptosis. Third, both studies have detected the appearances of the 35- and 25-kD C-terminal fragments of TDP-43 along the course of the pathogenesis development. Finally, Wils et al. (2010) used the Thy-1 promoter to direct the TDP-43 overexpression in the mice, which is active in a wider range of different types of cells, including neurons of the central nervous system, the muscle cells, the immune T cells, etc., and they characterized mainly the motor neuron dysfunction– and muscle defect–related pathology and behavioral phenotypes of the Tg mice, such as the spastic paralysis, muscle wasting, reduced movement, etc. However, use of the forebrain neuron–specific CaMKII promoter in our study has allowed the detection and follow up of pathogenesis development of the cognitive behaviors and motor function of the mice from their youth to over 2 yr of age. In addition, several hallmarks of FTLD-U, including the cognitive dysfunction, the hippocampal atrophy, and the progressive appearances of the 35- and 25-kD fragments and the high molecular weight species of TDP-43 in the urea-soluble fraction of the disease forebrains (Table I) could be observed in these mice. Thus, although the mice generated by Wils et al. (2010) are more suitable for studies of neurodegeneration reminiscent of ALS, our CaMKII-TDP-43 Tg mice are ideal for future detailed pathological/clinical analysis and drug/therapeutic development for FTLD-U.

MATERIALS AND METHODS

Construction and generation of CaMKII-TDP-43 Tg mice. To generate the Tg mice of FVB/N background, a 1,245-bp full-length mouse TDP-43 cDNA (available from GenBank/EMBL/DDBJ under accession no. NM_145556) was cloned into the EcoRV site of pNN265, a modified form of pcDNAI/Amp provided by E. Kandel (Columbia University, New York, NY; Mayford et al., 1996). A 2.7-kb NotI fragment was isolated from pNN265 and cloned into the NotI site of the vector pMM403 containing 8.5 kb of the mouse CaMKII promoter region (also provided by E. Kandel; Mayford et al., 1996), resulting in pCaMKII-TDP-43. An 11.2-kb SfiI fragment

was then purified from pCaMKII-TDP-43 and injected into the one-cell embryos of FVB/N mice. The injected embryos were then transferred into the oviducts of surrogate mothers. 78 offsprings from the surrogate mother mice carrying the Cam KII-TDP-43 transgene-injected embryos were genotyped, and 10 of them were identified as the founders. These FVB/N founders were bred with WT FVB/N mice, and three of them were germline transmitted. Each of the three germlines transmitted, CamKII-TDP-43 Tg lines were set to littermate intercrosses within the line so to obtain three homozygous TDP-43 Tg mouse lines. The homozygosity was determined by Southern blotting, and the overexpression of TDP-43 was confirmed by quantitative RT-PCR and Western blotting analyses of the forebrain tissues from 2-mo-old mice. All the mice were bred at the Animal Facility of the Institute of Molecular Biology (IMB), Academia Sinica, Taiwan. They were housed in a room maintained on a 12 h/12 h light/dark cycle (light on at 7:00 a.m.) with continuous supply of food and water. Experimental procedures for handling the mice were approved by the Institutional Animal Care and Utilization Committee, Academia Sinica.

For genotyping of the founders, both Southern blot analysis and PCR were performed according to the standard procedures. For Southern blot analysis, the genomic tail DNAs were digested with KpnI and hybridized with a 543 bp NotI fragment from pGEMT-TDP-43 (Promega). The genomic DNAs of the Tg CaMKII-TDP-43 mice would give rise to a 4.4-kb fragment on the blot. For PCR, the following primers were used: forward primer 5′-GGCTTGAGATCTGGCCATACACT-3′ and reverse primer 5′-TAAGATCTTTCTTGACCTGAACCATA-3′. A 523-bp band on gel was expected for the Tg mice, but not the WT or NT mice. The breeding test was used to confirm the homozygosity of the $Tg^{+/+}$ mice.

In situ hybridization. In situ hybridization was performed as described previously (Tsai et al., 2002), with minor modifications. 20-µm coronal sections were taken from the mouse brains serially, covering both the hippocampus and cortex of the cerebrum. The antisense probe complementary to the sequence of the TDP-43 mRNA (5′-GCTCTGAATGGTTTGGGAATGAAGACATCTACCACT-3′) and the corresponding sense probe were 3′ end-labeled with α-[^{35}S]dATP and hybridized, respectively, at 42°C for 24 h with Poly-Prep slides (Sigma-Aldrich) containing the brain sections. After extensive washing, the slides were dehydrated with ethanol and exposed to BioMax films (Kodak) for 10 d. The signals from the in situ hybridization were quantified by measuring the optic densities of the relevant fields with the use of the ImageJ program (National Institutes of Health).

Morris water maze task. For spatial learning test, the Morris water maze task was performed as described previously (Tsai et al., 2007). The animals were subjected to four trials per session and two sessions a day, with one session given in the morning and the other given in the afternoon. For a complete test, a total of 6 sessions in 3 d were given. The time spent by the individual mice to reach the platform in the water was recorded as the escape latency.

Fear conditioning task. For fear conditioning task, the mice were placed in a fear conditioning shock chamber (10 × 10 × 15 inches high) with multiparameter activity monitors. The conditioned stimulus (CS) used was an 85-dB sound at 2,800 Hz, and the unconditioned stimulus (US) was a continuous scrambled foot shock at 0.75 mA.

Locomotor activity. Mouse movement was monitored by the TRuScan Digiscan system (Coulbourn Instruments, Inc.), which uses infrared beams to detect the horizontal and vertical movements. The pattern of the beam breaks was computerized to generate a quantitative measure of the locomotor activity. Each mouse was placed in the testing chamber for 5 min for adaptation, followed by a 30-min recording for analysis of the total time moved.

Limb-clasping observation and rotarod test. The limb-clasping and rotarod tests were performed according to the procedures described by Hara et al. (2006). For the latter, the mice were placed on a rod rotating at 20 r.p.m., and the time taken for them to fall from the rod was measured. If a mouse stayed on the rod until the end of the 2 min trial, a time of 120 s was recorded.

Novel object recognition task. The experimental protocol previously described by Cao et al. (2008) was used. In brief, the mice were individually habituated to an open-field box for 3 d. During the training sessions, two novel objects were placed in the open field, and the animals were allowed to explore for 15 min. The time spent exploring each object was recorded. During the one-hour recall tests, the animals were placed back into the same box, in which one of the familiar objects from training was replaced by a novel object, and allowed to explore freely again for 15 min. The ratio of the time spent exploring any one of the two original objects (training session) or the novel object over the total time spent exploring both objects was used to measure the recognition function.

Western blotting. For analysis of the expression levels of different proteins (Fig. 1 C and Fig. 4 A), the extracts were prepared from the cerebral cortex, hippocampus, cerebellum, and spinal cord of the WT and male Tg mice of the age 2 mo by homogenization of the tissues in RIPA lysis buffer (50 mM Tris-HCl, 150 mM NaCl, 1% Igepal CA-630, 2 mM EDTA, pH 8.0, 1 mM Na_3VO4, 20 µg/ml pepstatin A, 20 µg/ml leupeptin, 20 µg/ml aprotinin, 1 mM PMSF, 50 mM NaF). The extracts were then analyzed by 8–12% SDS-PAGE, followed by blot hybridization with one or more of the following antibodies: a homemade anti-TDP-43 (Wang et al., 2008a), antitubulin (Millipore), anti-CamKII (Millipore), anti-ERK (Millipore), anti-pERK (Millipore), anti-pCREB (Millipore), anti-GAD67 (Millipore), anti-GAP43 (Millipore), anti-GFAP (Millipore), anti–protein kinase A (Millipore), and anti-*PGRN* (R&D Systems), respectively. The relative intensities of the bands were normalized against that of the tubulin and expressed as means ± SEM.

For the sequential biochemical fractionation analysis, the forebrain tissue was dissected, weighed, and sequentially extracted with buffers of increasing strength as previously described (Neumann et al., 2006). In brief, the forebrains were extracted sequentially at 5 ml/g (vol/wt) with low-salt (LS) buffer (10 mM Tris, pH 7.5, 5 mM EDTA, 1 mM DTT, 10% sucrose, and a cocktail of protease inhibitors), high-salt Triton X-100 (TX) buffer (LS + 1% Triton X-100 + 0.5 M NaCl), myelin floatation buffer (TX buffer containing 30% sucrose), and sarkosyl (SARK) buffer (LS + 1% N-Lauroylsarcosine + 0.5 M NaCl). The SARK-insoluble materials were further extracted in 0.25 ml/g urea buffer (7 M urea, 2 M thiourea, 4% 3-[(3-Cholamidopropyl)dimethylammonio]-1-propanesulfonate, 30 mM Tris, pH 8.5). The proteins in the urea-soluble samples were resolved by Tris-glycine/12% SDS-PAGE, transferred to nitrocellulose, and then probed with an anti-TDP antibody (Protein Tech Group) that was used in similar experiments (Winton et al., 2008).

Immunostaining. Immunostaining was used to examine the expression patterns of TDP-43 and GAD67 in primary hippocampal neuron cultures of the WT and Tg mice. Cells were dissected from embryonic day 16.5 embryos for culturing in Neuralbasal medium, and the cultured cells (DIV 14) were fixed with 4% paraformaldehyde (PFA). For staining, the cell were incubated overnight with the individual primary antibodies against GAD67 (1:500) and TDP-43 (1:100), respectively, in 1% donkey serum (D9663, Sigma) in PBS (phosphate buffered saline).

For immunofluorescence staining of the mouse brains, adult mice were anesthetized and perfused transcardially in PBS with 4% PFA. The brain was removed and then immersed in 4% PFA solution with 20% sucrose overnight. 12-µm-thick sections were incubated with one or more of the following: anti–TDP-43 antibody (one was previously generated in our laboratory [Wang et al., 2008b] and another was obtained from the Protein Tech Group), mouse monoclonal anti-GFAP (Millipore), mouse monoclonal anti-ubiquitin (Millipore), mouse monoclonal anti-NeuN (Millipore), and the Alexa Fluor 488–conjugated goat anti–mouse antibodies (Invitrogen). The sections were then incubated with DAPI and coverslipped with the mounting medium (fluorescent mounting medium; Dako). All sections were examined in a laser scanning confocal microscope (LSM 510; Carl Zeiss, Inc.).

Electrophysiological recordings. The brains of the WT and TDP-43 Tg mice of the age 2 mo were quickly removed and placed in cold cutting buffer. The hippocampus was sliced into 400-μm sections, submerged in artificial CSF (aCSF) buffer, and maintained for 1.5 h before recording. A bipolar tungsten-stimulating electrode was placed in the middle of the stratum radiatum layer of CA1 area, and the extracellular field potentials were recorded by a glass microelectrode (3 MΩ; filled with aCSF). The pulse duration was 100 μs, and the test responses were elicited at 0.05 Hz (GS-3200; Gould).

LTP was induced by two trains of 100 Hz stimulation each lasting for 1 s with a 20-s interval between them. The stimulation strength was set to provide field EPSPs (fEPSPs) with an amplitude that was 40–60% of the maximum. When the paired-pulse facilitation (PPF) was examined in the CA1 area, the stimulation was delivered at 0.01 Hz at interstimulus intervals of 20, 50, 80, 100, 200, 300, 400, and 500 ms, with the stainless-steel bipolar electrodes placed in the outer and inner molecular layers, respectively, of the piriform cortex. fEPSPs from the corresponding layers were recorded via the glass pipettes, and they were amplified and filtered at 1 kHz. The PPF ratio was calculated by dividing the amplitude of the second fEPSP by that of the first fEPSP.

Whole-cell voltage clamp recordings were performed on the hippocampal neurons cultured for 12–15 d using an Axopatch 200B amplifier (Molecular Devices). For the miniature post-synaptic current (mEPSC) experiments, 1 μM tetrodotoxin was added to the bath to suppress the action potentials. Only cells that had a resting membrane potentials less than −50 mV, stable capacitance, and resistance throughout the experiment were considered. The data recorded were digitized with Digidata 1322A (Molecular Devices) and analyzed with Clampfit 9.2 (Molecular Devices).

GABA analysis. To measure the brain GABA levels, the mouse brains were quickly dissected on a chilled dissection board, homogenized on ice (50 mg of tissue with 1 ml of 400 mM $HClO_4$ and 50 μM EDTA), and neutralized with 100 mM borate buffer (1:10). The homogenates were then centrifuged (14,000 rpm, 15 min, 4°C) and filtered with Ultrafree-MC centrifugal filter units (Millipore, 14000 rpm, 1 min, 4°C). The concentrations of GABA were then determined by HPLC.

MRI measurement. MRI was acquired in a 7.0 Tesla MRI system (Bruker Companies). High resolution T2-weighted images were acquired for the whole brain region of each mouse using a 3D-RARE (Rapid Acquisition with Relaxation Enhancement) sequence with a field of view of 200 × 150 × 100 mm^3 and a matrix size of 200 × 150 × 65 mm^3, yielding a voxel size of 100 × 100 × 154 μm^3. The repetition time (TR) and the echo time (TE) were 2,500 and 32 ms, respectively. The region of the hippocampus was selected manually from slice to slice, and the volume was then calculated by a homemade code using the MATLAB.

Neuronal counts. To quantitate and compare the numbers of the cortical neurons among the WT and Tg mice, comparable coronal brain sections derived from the septo-striatal, septo-diencephalic, or the caudal diencephalon regions of the cerebral cortexes were immunostained with antibody (anti-NeuN) against the neuronal marker NeuN. The numbers of neurons in a total of six comparable areas (2–3 adjacent fields for each area) were counted. The neuronal counts for the Tg mice were then normalized to the WT mice (100%).

TUNEL assay. For TUNEL assay, trypsinized brain sections were reattached on 0.01% polylysine-coated slides, fixed with 4% formaldehyde solution, and fluorescence stained following the protocols of the DeadEnd fluorometric TUNEL system (Promega). The stained samples were analyzed under a fluorescence microscope, and the signals counted in randomly selected views.

Survival analysis. The WT and the TDP-43 $Tg^{+/+}$ mice born between March 2006 and December 2008 were used to compare the lifespan/survival rates. Five of the animals per cage were maintained in a pathogen-free environment at the Animal Facility of the Institute of Molecular Biology, Academia Sinica, Taiwan. The dates of birth and death of each mouse were recorded. The survival curves were drawn by the Kaplan and Meier method, and compared by the Log-rank test.

Statistical analysis. All data are reported as the mean ± SEM. Independent experiments were compared by the Student's *t* test. Differences, indicated by the asterisks, were considered statistically significant at $P < 0.05$.

Online supplemental material. Fig. S1 shows the levels of TDP-43 in the TDP-43 $Tg^{+/+}$ and $Tg^{+/-}$ mice in comparison to the WT. Fig. S2 shows the water maze tests of CaMKII-TDP-43 $Tg^{+/-}$ mice in comparison to the WT, NT, and TDP-43 $Tg^{+/+}$ mice. Fig. S3 shows the survival curves of the TDP-43 $Tg^{+/+}$ and WT mice. Fig. S4 shows the histological analysis of the motor neurons in TDP-43 $Tg^{+/+}$ mice. Online supplemental material is available at http://www.jem.org/cgi/content/full/jem.20092164/DC1.

We thank three reviewers for their insightful and constructive suggestions. We also thank the Transgenic Core Facility in the Institute of Molecular Biology for the generation of the transgenic mice.

This study was supported by the Academia Sinica (AS), Taipei, Taiwan. K.-J. Tsai was an AS Postdoctoral Fellow and C.-K. J. Shen is an AS Investigator Awardee.

The authors have no conflicting financial interests.

Submitted: 7 October 2009
Accepted: 28 June 2010

REFERENCES

Alvarez-Saavedra, M., M.A. Sáez, D. Kang, H.Y. Zoghbi, and J.I. Young. 2007. Cell-specific expression of wild-type MeCP2 in mouse models of Rett syndrome yields insight about pathogenesis. *Hum. Mol. Genet.* 16:2315–2325. doi:10.1093/hmg/ddm185

Arai, T., M. Hasegawa, H. Akiyama, K. Ikeda, T. Nonaka, H. Mori, D. Mann, K. Tsuchiya, M. Yoshida, Y. Hashizume, and T. Oda. 2006. TDP-43 is a component of ubiquitin-positive tau-negative inclusions in frontotemporal lobar degeneration and amyotrophic lateral sclerosis. *Biochem. Biophys. Res. Commun.* 351:602–611. doi:10.1016/j.bbrc.2006.10.093

Ayala, Y.M., T. Misteli, and F.E. Baralle. 2008. TDP-43 regulates retinoblastoma protein phosphorylation through the repression of cyclin-dependent kinase 6 expression. *Proc. Natl. Acad. Sci. USA.* 105:3785–3789. doi:10.1073/pnas.0800546105

Barnes, J., J.L. Whitwell, C. Frost, K.A. Josephs, M. Rossor, and N.C. Fox. 2006. Measurements of the amygdala and hippocampus in pathologically confirmed Alzheimer disease and frontotemporal lobar degeneration. *Arch. Neurol.* 63:1434–1439. doi:10.1001/archneur.63.10.1434

Bose, J.K., I.F. Wang, L. Hung, W.Y. Tarn, and C.K. Shen. 2008. TDP-43 overexpression enhances exon 7 inclusion during the survival of motor neuron pre-mRNA splicing. *J. Biol. Chem.* 283:28852–28859. doi:10.1074/jbc.M805376200

Buratti, E., and F.E. Baralle. 2001. Characterization and functional implications of the RNA binding properties of nuclear factor TDP-43, a novel splicing regulator of CFTR exon 9. *J. Biol. Chem.* 276:36337–36343. doi:10.1074/jbc.M104236200

Buratti, E., and F.E. Baralle. 2008. Multiple roles of TDP-43 in gene expression, splicing regulation, and human disease. *Front. Biosci.* 13:867–878. doi:10.2741/2727

Cairns, N.J., M. Neumann, E.H. Bigio, I.E. Holm, D. Troost, K.J. Hatanpaa, C. Foong, C.L. White III, J.A. Schneider, H.A. Kretzschmar, et al. 2007. TDP-43 in familial and sporadic frontotemporal lobar degeneration with ubiquitin inclusions. *Am. J. Pathol.* 171:227–240. doi:10.2353/ajpath.2007.070182

Cao, X., H. Wang, B. Mei, S. An, L. Yin, L.P. Wang, and J.Z. Tsien. 2008. Inducible and selective erasure of memories in the mouse brain via chemical-genetic manipulation. *Neuron.* 60:353–366. doi:10.1016/j.neuron.2008.08.027

Carlezon, W.A. Jr., R.S. Duman, and E.J. Nestler. 2005. The many faces of CREB. *Trends Neurosci.* 28:436–445. doi:10.1016/j.tins.2005.06.005

Chen-Plotkin, A.S., F. Geser, J.B. Plotkin, C.M. Clark, L.K. Kwong, W. Yuan, M. Grossman, V.M. Van Deerlin, J.Q. Trojanowski, and

V.M. Lee. 2008. Variations in the progranulin gene affect global gene expression in frontotemporal lobar degeneration. *Hum. Mol. Genet.* 17:1349–1362. doi:10.1093/hmg/ddn023

Corrado, L., A. Ratti, C. Gellera, E. Buratti, B. Castellotti, Y. Carlomagno, N. Ticozzi, L. Mazzini, L. Testa, F. Taroni, et al. 2009. High frequency of TARDBP gene mutations in Italian patients with amyotrophic lateral sclerosis. *Hum. Mutat.* 30:688–694. doi:10.1002/humu.20950

Elman, L.B., L. McCluskey, and M. Grossman. 2008. Motor neuron disease and frontotemporal lobar degeneration: a tale of two disorders linked to TDP-43. *Neurosignals.* 16:85–90. doi:10.1159/000109762

Forman, M.S., J. Farmer, J.K. Johnson, C.M. Clark, S.E. Arnold, H.B. Coslett, A. Chatterjee, H.I. Hurtig, J.H. Karlawish, H.J. Rosen, et al. 2006. Frontotemporal dementia: clinicopathological correlations. *Ann. Neurol.* 59:952–962. doi:10.1002/ana.20873

Forman, M.S., J.Q. Trojanowski, and V.M. Lee. 2007. TDP-43: a novel neurodegenerative proteinopathy. *Curr. Opin. Neurobiol.* 17:548–555. doi:10.1016/j.conb.2007.08.005

Giordana, M.T., M. Piccinini, S. Grifoni, G. De Marco, M. Vercellino, M. Magistrello, A. Pellerino, B. Buccinnà, E. Lupino, and M.T. Rinaudo. 2010. TDP-43 redistribution is an early event in sporadic amyotrophic lateral sclerosis. *Brain Pathol.* 20:351–360. doi:10.1111/j.1750-3639.2009.00284.x

Hara, T., K. Nakamura, M. Matsui, A. Yamamoto, Y. Nakahara, R. Suzuki-Migishima, M. Yokoyama, K. Mishima, I. Saito, H. Okano, and N. Mizushima. 2006. Suppression of basal autophagy in neural cells causes neurodegenerative disease in mice. *Nature.* 441:885–889. doi:10.1038/nature04724

Hernández-Sánchez, C., A.S. Basile, I. Fedorova, H. Arima, B. Stannard, A.M. Fernandez, Y. Ito, and D. LeRoith. 2001. Mice transgenically overexpressing sulfonylurea receptor 1 in forebrain resist seizure induction and excitotoxic neuron death. *Proc. Natl. Acad. Sci. USA.* 98:3549–3554. doi:10.1073/pnas.051012898

Hodges, J.R., R.R. Davies, J.H. Xuereb, B. Casey, M. Broe, T.H. Bak, J.J. Kril, and G.M. Halliday. 2004. Clinicopathological correlates in frontotemporal dementia. *Ann. Neurol.* 56:399–406. doi:10.1002/ana.20203

Johnson, B.S., J.M. McCaffery, S. Lindquist, and A.D. Gitler. 2008. A yeast TDP-43 proteinopathy model: Exploring the molecular determinants of TDP-43 aggregation and cellular toxicity. *Proc. Natl. Acad. Sci. USA.* 105:6439–6444. doi:10.1073/pnas.0802082105

Kabashi, E., P.N. Valdmanis, P. Dion, D. Spiegelman, B.J. McConkey, C. Vande Velde, J.P. Bouchard, L. Lacomblez, K. Pochigaeva, F. Salachas, et al. 2008. TARDBP mutations in individuals with sporadic and familial amyotrophic lateral sclerosis. *Nat. Genet.* 40:572–574. doi:10.1038/ng.132

Kandel, E.R. 2001. The molecular biology of memory storage: a dialogue between genes and synapses. *Science.* 294:1030–1038. doi:10.1126/science.1067020

Kertesz, A., T. Kawarai, E. Rogaeva, P. St George-Hyslop, P. Poorkaj, T.D. Bird, and D.G. Munoz. 2000. Familial frontotemporal dementia with ubiquitin-positive, tau-negative inclusions. *Neurology.* 54:818–827.

Kida, S., S.A. Josselyn, S. Peña de Ortiz, J.H. Kogan, I. Chevere, S. Masushige, and A.J. Silva. 2002. CREB required for the stability of new and reactivated fear memories. *Nat. Neurosci.* 5:348–355. doi:10.1038/nn819

Kwong, L.K., M. Neumann, D.M. Sampathu, V.M. Lee, and J.Q. Trojanowski. 2007. TDP-43 proteinopathy: the neuropathology underlying major forms of sporadic and familial frontotemporal lobar degeneration and motor neuron disease. *Acta Neuropathol.* 114:63–70. doi:10.1007/s00401-007-0226-5

Lagier-Tourenne, C., and D.W. Cleveland. 2009. Rethinking ALS: the FUS about TDP-43. *Cell.* 136:1001–1004. doi:10.1016/j.cell.2009.03.006

Lillo, P., and J.R. Hodges. 2009. Frontotemporal dementia and motor neurone disease: overlapping clinic-pathological disorders. *J. Clin. Neurosci.* 16:1131–1135. doi:10.1016/j.jocn.2009.03.005

Lomen-Hoerth, C., T. Anderson, and B. Miller. 2002. The overlap of amyotrophic lateral sclerosis and frontotemporal dementia. *Neurology.* 59:1077–1079.

Mackenzie, I.R., and R. Rademakers. 2008. The role of transactive response DNA-binding protein-43 in amyotrophic lateral sclerosis and frontotemporal dementia. *Curr. Opin. Neurol.* 21:693–700. doi:10.1097/WCO.0b013e3283168d1d

Mackenzie, I.R., A. Baborie, S. Pickering-Brown, D. Du Plessis, E. Jaros, R.H. Perry, D. Neary, J.S. Snowden, and D.M. Mann. 2006. Heterogeneity of ubiquitin pathology in frontotemporal lobar degeneration: classification and relation to clinical phenotype. *Acta Neuropathol.* 112:539–549. doi:10.1007/s00401-006-0138-9

Mangiarini, L., K. Sathasivam, M. Seller, B. Cozens, A. Harper, C. Hetherington, M. Lawton, Y. Trottier, H. Lehrach, S.W. Davies, and G.P. Bates. 1996. Exon 1 of the HD gene with an expanded CAG repeat is sufficient to cause a progressive neurological phenotype in transgenic mice. *Cell.* 87:493–506. doi:10.1016/S0092-8674(00)81369-0

Martinac, J.A., D.K. Craft, J.H. Su, R.C. Kim, and C.W. Cotman. 2001. Astrocytes degenerate in frontotemporal dementia: possible relation to hypoperfusion. *Neurobiol. Aging.* 22:195–207. doi:10.1016/S0197-4580(00)00231-1

Mayford, M., M.E. Bach, Y.Y. Huang, L. Wang, R.D. Hawkins, and E.R. Kandel. 1996. Control of memory formation through regulated expression of a CaMKII transgene. *Science.* 274:1678–1683. doi:10.1126/science.274.5293.1678

Mishra, M., T. Paunesku, G.E. Woloschak, T. Siddique, L.J. Zhu, S. Lin, K. Greco, and E.H. Bigio. 2007. Gene expression analysis of frontotemporal lobar degeneration of the motor neuron disease type with ubiquitinated inclusions. *Acta Neuropathol.* 114:81–94. doi:10.1007/s00401-007-0240-7

Moisse, K., J. Mepham, K. Volkening, I. Welch, T. Hill, and M.J. Strong. 2009a. Cytosolic TDP-43 expression following axotomy is associated with caspase 3 activation in NFL−/− mice: support for a role for TDP-43 in the physiological response to neuronal injury. *Brain Res.* 1296:176–186. doi:10.1016/j.brainres.2009.07.023

Moisse, K., K. Volkening, C. Leystra-Lantz, I. Welch, T. Hill, and M.J. Strong. 2009b. Divergent patterns of cytosolic TDP-43 and neuronal progranulin expression following axotomy: implications for TDP-43 in the physiological response to neuronal injury. *Brain Res.* 1249:202–211. doi:10.1016/j.brainres.2008.10.021

Neary, D., J.S. Snowden, L. Gustafson, U. Passant, D. Stuss, S. Black, M. Freedman, A. Kertesz, P.H. Robert, M. Albert, et al. 1998. Frontotemporal lobar degeneration: a consensus on clinical diagnostic criteria. *Neurology.* 51:1546–1554.

Neumann, M. 2009. Molecular neuropathology of TDP-43 proteinopathies. *Int. J. Mol. Sci.* 10:232–246. doi:10.3390/ijms10010232

Neumann, M., D.M. Sampathu, L.K. Kwong, A.C. Truax, M.C. Micsenyi, T.T. Chou, J. Bruce, T. Schuck, M. Grossman, C.M. Clark, et al. 2006. Ubiquitinated TDP-43 in frontotemporal lobar degeneration and amyotrophic lateral sclerosis. *Science.* 314:130–133. doi:10.1126/science.1134108

Neumann, M., L.K. Kwong, D.M. Sampathu, J.Q. Trojanowski, and V.M. Lee. 2007. TDP-43 proteinopathy in frontotemporal lobar degeneration and amyotrophic lateral sclerosis: protein misfolding diseases without amyloidosis. *Arch. Neurol.* 64:1388–1394. doi:10.1001/archneur.64.10.1388

O'Leary, D.D., S.J. Chou, and S. Sahara. 2007. Area patterning of the mammalian cortex. *Neuron.* 56:252–269. doi:10.1016/j.neuron.2007.10.010

Ou, S.H., F. Wu, D. Harrich, L.F. García-Martínez, and R.B. Gaynor. 1995. Cloning and characterization of a novel cellular protein, TDP-43, that binds to human immunodeficiency virus type 1 TAR DNA sequence motifs. *J. Virol.* 69:3584–3596.

Ratnavalli, E., C. Brayne, K. Dawson, and J.R. Hodges. 2002. The prevalence of frontotemporal dementia. *Neurology.* 58:1615–1621.

Ridet, J.L., S.K. Malhotra, A. Privat, and F.H. Gage. 1997. Reactive astrocytes: cellular and molecular cues to biological function. *Trends Neurosci.* 20:570–577. doi:10.1016/S0166-2236(97)01139-9

Snowden, J., D. Neary, and D. Mann. 2007. Frontotemporal lobar degeneration: clinical and pathological relationships. *Acta Neuropathol.* 114:31–38. doi:10.1007/s00401-007-0236-3

Tan, C.F., Y.S. Piao, A. Kakita, M. Yamada, H. Takano, M. Tanaka, A. Mano, K. Makino, M. Nishizawa, K. Wakabayashi, and H. Takahashi. 2005. Frontotemporal dementia with co-occurrence of astrocytic plaques and tufted astrocytes, and severe degeneration of the cerebral white matter:

a variant of corticobasal degeneration? *Acta Neuropathol.* 109:329–338. doi:10.1007/s00401-004-0933-0

Tang, Y.P., E. Shimizu, G.R. Dube, C. Rampon, G.A. Kerchner, M. Zhuo, G. Liu, and J.Z. Tsien. 1999. Genetic enhancement of learning and memory in mice. *Nature.* 401:63–69. doi:10.1038/43432

Tsai, K.J., S.K. Chen, Y.L. Ma, W.L. Hsu, and E.H. Lee. 2002. sgk, a primary glucocorticoid-induced gene, facilitates memory consolidation of spatial learning in rats. *Proc. Natl. Acad. Sci. USA.* 99:3990–3995. doi:10.1073/pnas.062405399

Tsai, K.J., Y.C. Tsai, and C.K.J. Shen. 2007. G-CSF rescues the memory impairment of animal models of Alzheimer's disease. *J. Exp. Med.* 204:1273–1280. doi:10.1084/jem.20062481

Vossel, K.A., and B.L. Miller. 2008. New approaches to the treatment of frontotemporal lobar degeneration. *Curr. Opin. Neurol.* 21:708–716. doi:10.1097/WCO.0b013e328318444d

Wang, I.F., N.M. Reddy, and C.K.J. Shen. 2002. Higher order arrangement of the eukaryotic nuclear bodies. *Proc. Natl. Acad. Sci. USA.* 99:13583–13588. doi:10.1073/pnas.212483099

Wang, H.Y., I.F. Wang, J. Bose, and C.K.J. Shen. 2004. Structural diversity and functional implications of the eukaryotic TDP gene family. *Genomics.* 83:130–139. doi:10.1016/S0888-7543(03)00214-3

Wang, I.F., L.S. Wu, and C.K.J. Shen. 2008a. TDP-43: an emerging new player in neurodegenerative diseases. *Trends Mol. Med.* 14:479–485. doi:10.1016/j.molmed.2008.09.001

Wang, I.F., L.S. Wu, H.Y. Chang, and C.K.J. Shen. 2008b. TDP-43, the signature protein of FTLD-U, is a neuronal activity-responsive factor. *J. Neurochem.* 105:797–806. doi:10.1111/j.1471-4159.2007.05190.x

Weihl, C.C., P. Temiz, S.E. Miller, G. Watts, C. Smith, M. Forman, P.I. Hanson, V. Kimonis, and A. Pestronk. 2008. TDP-43 accumulation in inclusion body myopathy muscle suggests a common pathogenic mechanism with frontotemporal dementia. *J. Neurol. Neurosurg. Psychiatry.* 79:1186–1189. doi:10.1136/jnnp.2007.131334

Wils, H., G. Kleinberger, J. Janssens, S. Pereson, G. Joris, I. Cuijt, V. Smits, C.C. Groote, C. Van Broeckhoven, and S. Kumar-Singh. 2010. TDP-43 transgenic mice develop spastic paralysis and neuronal inclusions characteristic of ALS and frontotemporal lobar degeneration. *Proc. Natl. Acad. Sci. USA.* 107:3853–3863. doi:10.1073/pnas.0912417107

Winton, M.J., L.M. Igaz, M.M. Wong, L.K. Kwong, J.Q. Trojanowski, and V.M. Lee. 2008. Disturbance of nuclear and cytoplasmic TAR DNA-binding protein (TDP-43) induces disease-like redistribution, sequestration, and aggregate formation. *J. Biol. Chem.* 283:13302–13309. doi:10.1074/jbc.M800342200

Wu, L.S., W.C. Cheng, S.C. Hou, Y.T. Yan, S.T. Jiang, and C.K. Shen. 2010. TDP-43, a neuro-pathosignature factor, is essential for early mouse embryogenesis. *Genesis.* 48:56–62.

Zhang, Y.J., Y.F. Xu, C. Cook, T.F. Gendron, P. Roettges, C.D. Link, W.L. Lin, J. Tong, M. Castanedes-Casey, P. Ash, et al. 2009. Aberrant cleavage of TDP-43 enhances aggregation and cellular toxicity. *Proc. Natl. Acad. Sci. USA.* 106:7607–7612. doi:10.1073/pnas.0900688106